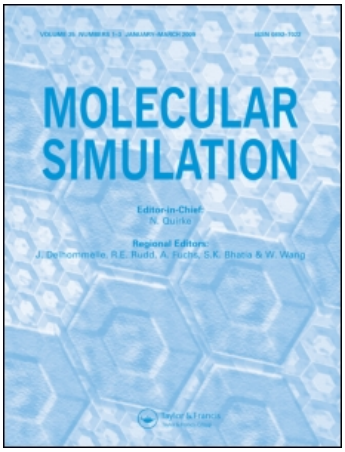

Molecular Simulation
Publication details, including instructions for authors and subscription information:
http://www.informaworld.com/smpp/title~content=t713644482

Molecular simulation of imidazolium amino acid-based ionic liquids

Xiaomin Liu[a]; Guohui Zhou[b]; Suojiang Zhang[a]; Guangwen Wu[c]
[a] State Key Laboratory of Multiphase Complex Systems, Institute of Process Engineering, Chinese Academy of Sciences, Beijing, P.R. China [b] Beijing Salien Machine Facility Ltd, Beijing, P.R. China [c] Center for Molecular Simulation, Swinburne University of Technology, Hawthorn, Vic., Australia

Online publication date: 10 December 2010

To cite this Article Liu, Xiaomin , Zhou, Guohui , Zhang, Suojiang and Wu, Guangwen(2010) 'Molecular simulation of imidazolium amino acid-based ionic liquids', Molecular Simulation, 36: 14, 1123 — 1130
To link to this Article: DOI: 10.1080/08927022.2010.497923
URL: http://dx.doi.org/10.1080/08927022.2010.497923

Molecular Simulation
Vol. 36, No. 14, December 2010, 1123–1130

Taylor & Francis
Taylor & Francis Group

Molecular simulation of imidazolium amino acid-based ionic liquids

Xiaomin Liu[a], Guohui Zhou[b], Suojiang Zhang[a]* and Guangwen Wu[c]

[a]*State Key Laboratory of Multiphase Complex Systems, Institute of Process Engineering, Chinese Academy of Sciences, Beijing 100190, P.R. China;* [b]*Beijing Salien Machine Facility Ltd, Beijing 100083, P.R. China;* [c]*Center for Molecular Simulation, Swinburne University of Technology, Hawthorn, Vic. 3122, Australia*

(*Received 25 February 2010; final version received 25 May 2010*)

A series of 1-alkyl-3-methylimidazolium amino acid ionic liquids (ILs) [$C_n$mim][Gly] were studied by molecular simulations based on the all-atom force field. Volume expansivity and heat capacities for [C_2mim][Gly] were calculated for validating the force field. Site-to-site and centre-of-mass radial distribution functions were investigated to depict the microscopic structures. It is interesting to find that one $[Gly]^-$ anion could catch more than two imidazolium rings, and they may arrange approximately parallel to each other. Moreover, aggregation of the alkyl chains was observed in the ILs with alkyl side chains longer than or equal to C4.

Keywords: molecular dynamics simulation; amino acid; ionic liquid

1. Introduction

Ionic liquids (ILs) have been attracting considerable attention due to their designable nature for a variety of potential applications [1–6]. In recent years, amino acid ILs, as an important kind of ILs, have been studied by more and more scientists. Fukumoto et al. [7] succeeded in synthesising ILs from 20 natural amino acids in 2005. Yang et al. [8] synthesised the amino acid IL, 1-ethyl-3-methylimidazolium aminoacetate ([C_2mim][Gly]), and measured the densities and surface tensions of [C_2-mim][Gly] at different temperatures. A new series of task-specific ILs, tetrabutylphosphonium amino acid ([$P(C_4)_4$][AA]), were synthesised by Zhang et al. [9] to capture CO_2, and CO_2 absorption capacity at equilibrium was 50 mol% of ILs. In various fields, including industrial chemistry and pharmaceutical chemistry, the amino acid ILs have proved to be useful in intermediates for peptide syntheses, functional materials and biodegradable ILs [7].

Molecular simulation is an indispensable tool for understanding the microstructures of the ILs [10–20]. For example, Wang and Voth [21] used the multiscale coarse-graining method and found the spatial heterogeneity in imidazolium-based ILs. Bhargava and Balasubramanian [22] performed the molecular simulation to study the structure of the liquid–vapour interface of [C_4mim][PF_6]. Maginn et al. [23] investigated the underlying mechanisms for the high solubility of CO_2 in imidazolium-based ILs and dramatic increase in viscosity after absorption of CO_2 in amine-functionalised ILs [24]. In this work, a serial of amino acid ILs were studied based on the force field of 1-alkyl-3-methylimidazolium ($[C_n mim]^+$) [14] and glycine ($[Gly]^-$) [25]. The restraint electrostatic potential (RESP) [26] method was used to obtain the point charges of $[C_n mim]^+$. Molecular dynamics (MD) simulations were carried out in the isothermal–isobaric ensemble for four kinds of 1-alkyl-3-methylimidazolium aminoacetate [$C_n$mim][Gly] ILs. The volume expansivities and heat capacities for [C_2mim][Gly] were calculated, and a good agreement with the experimental data was obtained. Moreover, the interaction between cations and anions was analysed by radial distribution functions (RDFs) of these ILs. Aggregation of the alkyl chains in non-polar domains was observed in the ILs with alkyl side chains longer than or equal to C4. Because one terminal of $[Gly]^-$ is the electronic acceptor, and the another is the adopter, hydrogen bonds between anions themselves were found. In addition, it is interesting to find that the imidazolium rings are aligned approximately parallel to each other, and the distance between the rings is very close, even closer than that between the ring and the anion.

*Corresponding author. Email: sjzhang@home.ipe.ac.cn

ISSN 0892-7022 print/ISSN 1029-0435 online

DOI: 10.1080/08927022.2010.497923
http://www.informaworld.com

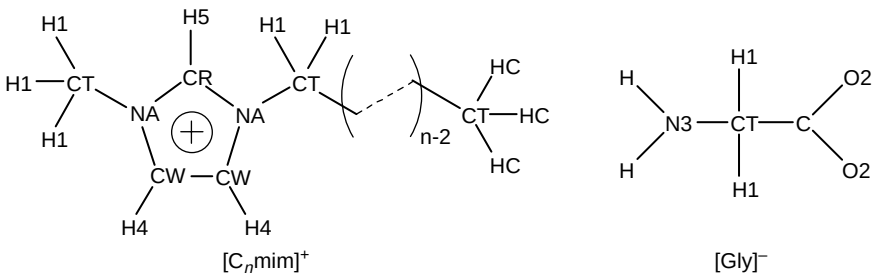

Figure 1. Structures and atom types of $[C_n\text{mim}]^+$ cations and the $[\text{Gly}]^-$ anion.

2. Force-field development

The AMBER force field [27] was used with the following functional form for the potential energy E:

$$E_{\text{total}} = \sum_{\text{bonds}} K_r(r - r_0)^2 + \sum_{\text{angles}} K_\theta(\theta - \theta_0)^2 + \sum_{\text{torsions}} \frac{K_\phi}{2}(1 + \cos(n\phi - \gamma)) + \sum_{i=1}^{N}\sum_{j=i+1}^{N}\left\{4\varepsilon_{ij}\left[\left(\frac{\sigma_{ij}}{r_{ij}}\right)^{12} - \left(\frac{\sigma_{ij}}{r_{ij}}\right)^{6}\right] + \frac{q_i q_j}{r_{ij}}\right\}, \quad (1)$$

where the potential parameters have their usual meaning. Lennard-Jones parameters for interactions between different atom types were obtained by using the Lorentz–Berthelot mixing rule [28]:

$$\varepsilon_{ij} = \sqrt{\varepsilon_{ii}\varepsilon_{jj}}, \quad \sigma_{ij} = (\sigma_{ii} + \sigma_{jj})/2. \quad (2)$$

The structures of $[C_n\text{mim}]^+$ were optimised at the B3LYP/6-31+G* level using the Gaussian 03 program. The atomic charges were fitted to reproduce the molecular electrostatic potential and calculated at the 6-311+G**/B3LYP level. The fitting was carried out using the RESP method. Atomic partial charges, the equilibrium bonds and angles obtained from the optimised structures are listed in Tables S1 and S2 (please refer to the supporting information, available online). The atom types for $[C_n\text{mim}]^+$ are presented in Figure 1.

3. Simulation details

MD simulations for all the four $[C_n\text{mim}][\text{Gly}]$ ILs were performed using the M.DynaMix program version 4.3 [29]. Each system contains 192 $[C_n\text{mim}]^+$ cations and 192 $[\text{Gly}]^-$ anions. Simulations started from the FCC lattice at a low density of 0.2 g/cm^3. After the system was relaxed in the NVE ensemble for a few MD steps (2000 steps) to remove the possible overlapping in the initial configuration, the Nosé–Hoover [30] NpT ensemble was adopted with coupling constants of 100 and 1000 fs for temperature and pressure, respectively. Then, the system density gradually increased. The Tuckerman–Berne double time-step algorithm [31] was employed with long and short time steps of 2 and 0.2 fs, respectively. The intramolecular forces were cut off at 15 Å, while the long-range forces, including LJ and Coulombic interactions, were cut off at 20 Å, and the Ewald [32] summation was implemented for the latter. The system equilibrated for at least 1.0 ns, and each production phase lasted for another 3.0 ns at 298.15 K under 1.0 atm.

4. Results and discussion

4.1 Liquid densities

Table 1 shows the computed densities of $[C_n\text{mim}][\text{Gly}]$ and experimental data for $[C_2\text{mim}][\text{Gly}]$ at different temperatures. The predicted densities of $[C_2\text{mim}][\text{Gly}]$ are higher than the experimental densities [8] by about 2.0%. The agreement is good considering that the calculations are purely predictive, which means the force field of

Table 1. Comparison of predicted and experimental density, molar volumes and volume expansivities at 1.0 atm.

		ρ (g/cm^3)		V (cm^3/mol)		α_P (10^{-4} K^{-1})	
IL	T (K)	Sim.	Exp.	Sim.	Exp.	Sim.	Exp.
–	298.15	1.179	1.1589	157.1	159.8	4.81	5.24
$[C_2\text{mim}][\text{Gly}]$	323.15	1.165	1.1437	159.0	162.0	4.76	5.17
–	343.15	1.154	1.1322	160.5	163.6	4.71	5.12
$[C_4\text{mim}][\text{Gly}]$	298.15	1.103	–	194.3	–	–	–
$[C_6\text{mim}][\text{Gly}]$	298.15	1.061	–	227.5	–	–	–
$[C_{10}\text{mim}][\text{Gly}]$	298.15	0.998	–	298.0	–	–	–

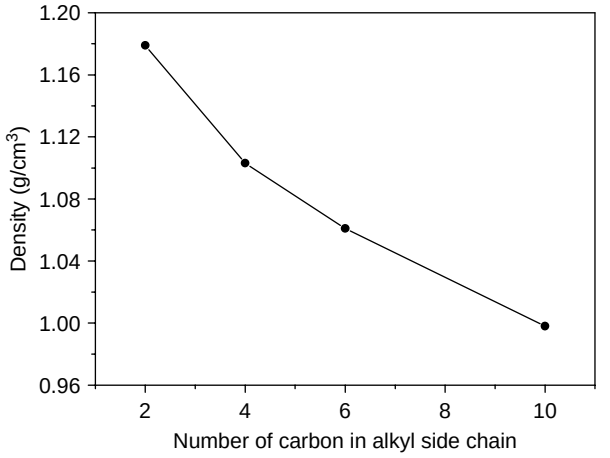

Figure 2. Density of [$C_n$mim][Gly] vs. number of carbon in the alkyl side chain.

$[C_n\text{mim}]^+$ and $[\text{Gly}]^-$ could be successfully used in this system. It can be seen in Figure 2 that the density of [$C_n$mim][Gly] reduces with the increase in the number of carbon in the alkyl side chain, and this result is similar to that of [$C_n$mim][TFSI] [33].

4.2 Volume expansivity

The volume expansivity quantifies the extent to which the volume of a fluid changes with temperature at constant pressure, and it is defined as [10]

$$\alpha_{\text{P}} = \frac{1}{V}\left(\frac{\partial V}{\partial T}\right)_{\text{P}}. \tag{3}$$

It is another important data for validating a proposed force-field except for density. The volume expansivity was obtained by running a series of simulations at different temperatures. As the change in volume with temperature is approximately linear (Figure 3), α_{P} can be calculated according to Equation (3) by fitting a straight line to the simulated molar volume. Table 1 lists the computed volume expansivities of [$C_n$mim][Gly]. Comparing with the experimental results, the simulated expansivities of [C_2mim][Gly] are bigger than the experimental values [8] by less than 2.0% in all cases, and the agreement is good enough to confirm that the proposed force field can be successfully used in this kind of ILs.

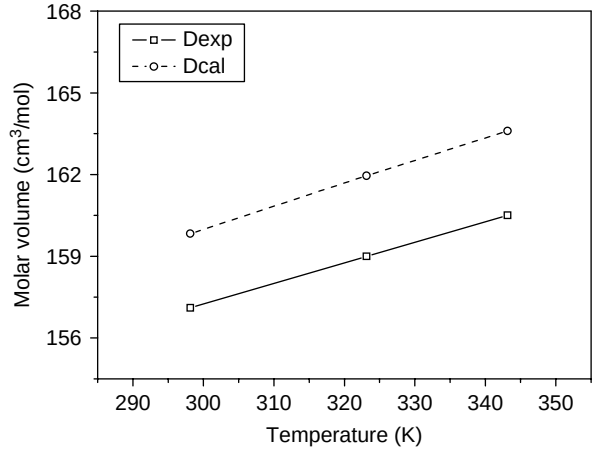

Figure 3. Molar volume of [C_2mim][Gly] vs. temperature.

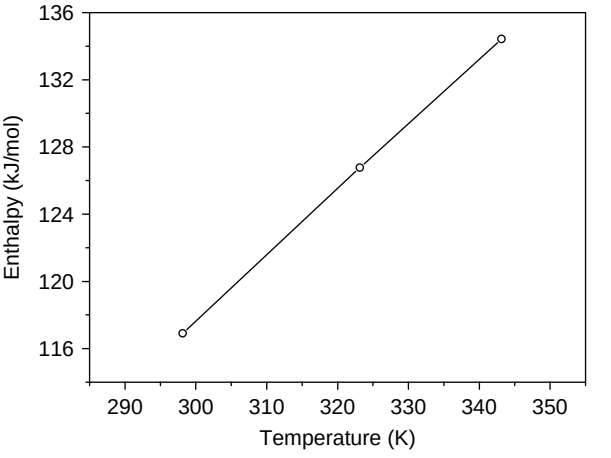

Figure 4. Enthalpy of [C_2mim][Gly] vs. temperature.

4.3 Heat capacity at constant pressure

The heat capacity at constant pressure can be calculated by [34]:

$$Cp(T,p) = \left(\frac{\partial H}{\partial T}\right)_p, \tag{4}$$

where H is the enthalpy.

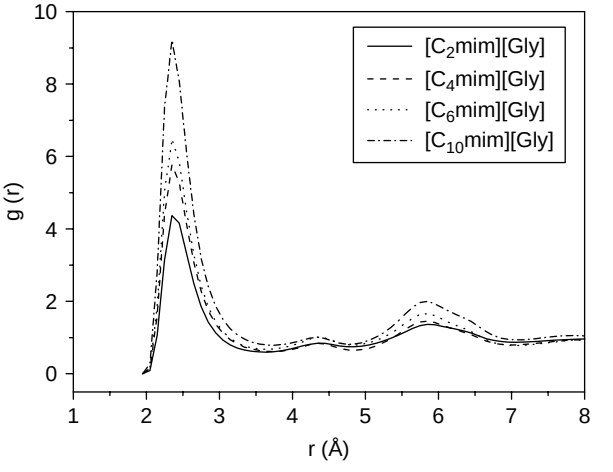

Figure 5. RDFs between H5 in [$C_n$mim] with O2 in [Gly].

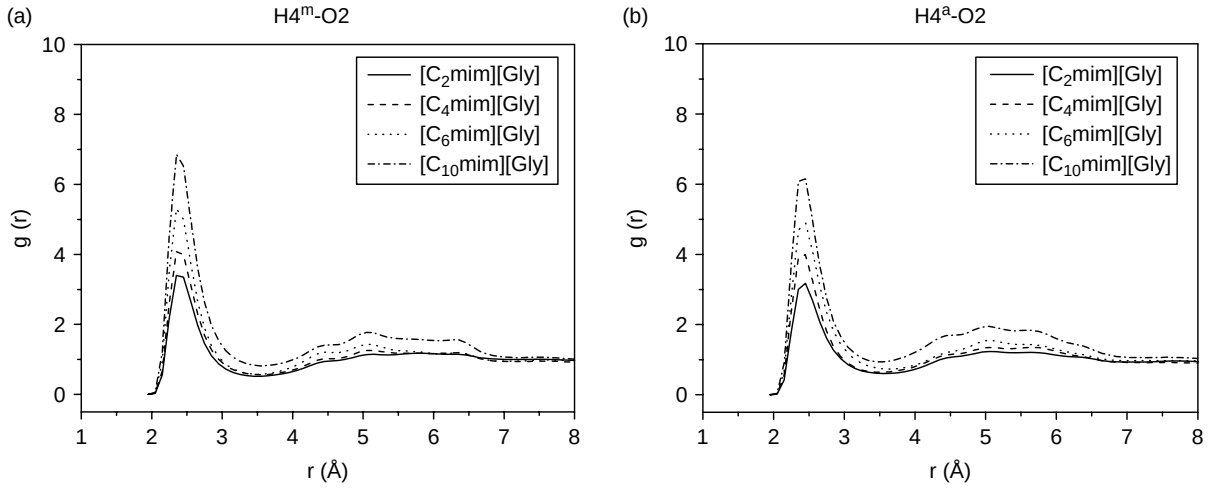

Figure 6. RDFs between $H4^m$ and $H4^a$ in [$C_n$mim] with O2 in [Gly].

$$H = E^{NB} + E^{INT} + K + pV. \quad (5)$$

The total potential energy E is split into non-bonded and intramolecular terms ($E = E^{NB} + E^{INT}$). K is the kinetic energy, p and V are the pressure and molar volume, respectively.

The heat capacity at constant pressure was computed under several temperatures and 1.0 atm. Because the change in enthalpy with temperature is approximately linear, C_P can be calculated using Equation (4) by fitting a straight line to the simulated enthalpy data (see Figure 4). The computed heat capacity between 298.15 and 343.15 K is 390 J mol^{-1} K^{-1} or 2.10 J g^{-1} K^{-1}, which is lower than the heat capacities of most tetrabutylphosphonium amino acid ILs [25], for example, the *Cp* of $[P(C_4)_4]$[Gly] is 2.525 J g^{-1} K^{-1} [25].

4.4 Micro-interaction and structure

4.4.1 Atomic interaction

To understand the effect of alkyl side chains on structures of [$C_n$mim][Gly], the RDFs between H atoms in the imidazolium ring of $[C_n mim]^+$ with O2 in $[Gly]^-$ were investigated. Figure 5 shows the RDFs between H5 and O2. All the first maximum locations of these RDFs are 2.35 Å, however, the peak height decreases with reducing the length of the alkyl side chain. It indicates that the activity of H5 in the cation with different alkyl side chains decreases in the order of $[C_{10}mim]^+ > [C_6mim]^+ > [C_4mim]^+ > [C_2mim]^+$.

Figure 6 shows the RDFs between H4 and O2 ($H4^m$ is the H atom close to the methyl, and $H4^a$ is the H atom close to the alkyl side chain). Both RDFs of $H4^m$—O2 and $H4^a$—O2 are similar to that of H5—O2, but a little lower.

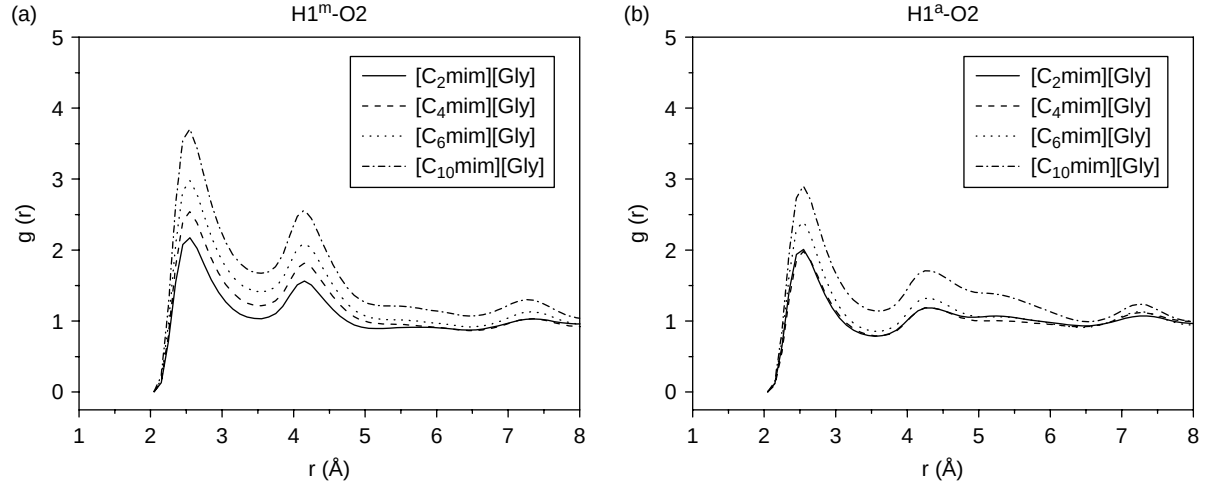

Figure 7. RDFs between $H1^m$ and $H1^a$ in [$C_n$mim] with O2 in [Gly].

Table 2. The first peak location of the RDFs between O2 and different H.

IL	H5	$H4^a$	$H4^b$	$H1^a$	$H1^b$
$[C_2mim][Gly]$	2.35	2.45	2.35	2.55	2.55
$[C_4mim][Gly]$	2.35	2.45	2.35	2.55	2.55
$[C_6mim][Gly]$	2.35	2.45	2.35	2.55	2.55
$[C_{10}mim][Gly]$	2.35	2.45	2.35	2.55	2.55

It indicated that the O2 prefers to distribute around H5, rather than H4 ($H4^m$ and $H4^a$). The first maximum locations of the RDFs are 2.45 and 2.35 Å for $H4^m$—O2 and $H4^a$—O2, respectively. Compared with $H4^m$—O2, the peak height of $H4^a$—O2 is little higher, and that might be caused by the larger atom charge of $H4^a$.

Interactions between O2 in $[Gly]^-$ and H1 in methyl and methylene connecting with the imidazolium ring were studied. RDFs for H1—O2 are shown in Figure 7, $H1^m$ and $H1^a$ are the H atom on methyl and methylene, respectively. The strength between H1 and O2 is lower than the H4—O2, and the similar varying regularity with changing the length of alkyl side chains is observed. It is found that activity of the different H atoms in the cation decreases in the order of H5 > H4 > H1. The first peak locations for $[C_n mim][Gly]$ are shown in Table 2, and it is obvious that the locations are the same for these ILs. The above results imply that the length of alkyl side chains has little effect on the atom interaction distance, but may change the interaction strength.

Wang and Voth [21] found the aggregation of the alkyl side chain in $[C_4mim][NO_3]$ using the multiscale coarse-graining method. Lopes and Pádua [12] studied the nanostructure organisation in $[C_n mim][PF_6]$ and $[C_n mim][(CF_3SO_2)_2N]$. In this work, the aggregation in $[C_n mim][Gly]$ was also discussed. For $[C_{10}mim]^+$, the end carbon is named C10, and in the order of approaching to the imidazolium ring it is C9, C8, …, C1. Figure 8 shows the RDFs between pairs of equivalent carbon atoms along the alkyl chain of $[C_{10}mim]^+$. It can be seen that the interaction between the end-methyl (C10) in the side chain is the strongest, and the interactions of the methylene decrease in the order of moving to the central imidazolium ring. In order to investigate the influence of the alkyl chain length on the interaction, RDFs between the terminal carbon of the alkyl chain for $[C_n mim]^+$ were studied and are shown in Figure 9. The peak heights of RDFs for three $[C_n mim]^+$, except $[C_2mim]^+$, are higher than 2.0, the present results agree with the ones reported by Lopes and Pádua [12].

4.4.2 *Ionic interaction*

Centre-of-mass (COM) RDFs are used to depict the ion interactions and to study the microstructures. First, the COM RDFs between the anion and the imidazolium ring (including adjacent atoms) are considered, and it is shown in Figure 10(ia). It can be seen that peaks of these RDFs are located at about 6 Å. Then, we calculated the COM RDFs for anion–anion, which are shown in Figure 10(aa). The highest peaks locate at about 9 Å. There is a small peak before the highest one, and these RDFs are not similar to those reported results for $[PF_6]^-$[14]. We suppose that it may be caused by the weak hydrogen bond interaction between O2 and H of amino acid in different anions. In order to check the interaction, RDFs of O2—H were studied and are shown in Figure 11. Because of the small radius and big atom charge of H, these RDFs are sharp but narrow, which may imply the existence of the hydrogen bond but of weak interaction.

The cation–cation COM RDFs are shown in Figure 10(cc). In these RDFs, no clear peak is found. It is reported that the imidazolium ring, plus the CH_2 and CH_3 bonded directly to it compose the charged domains [12].

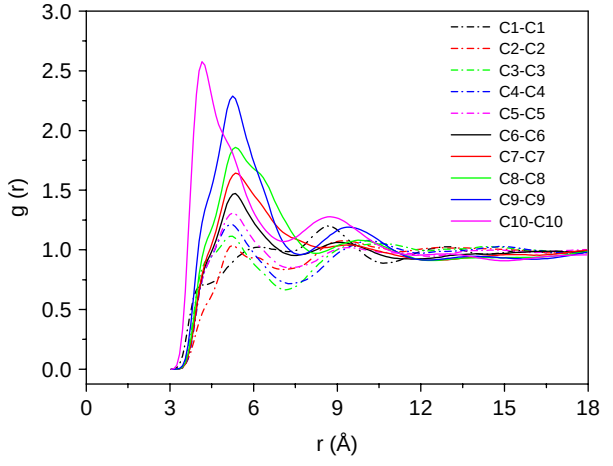

Figure 8. Intermolecular atom–atom RDFs between several equivalent carbons along the alkyl side chain in $[C_{10}mim][Gly]$.

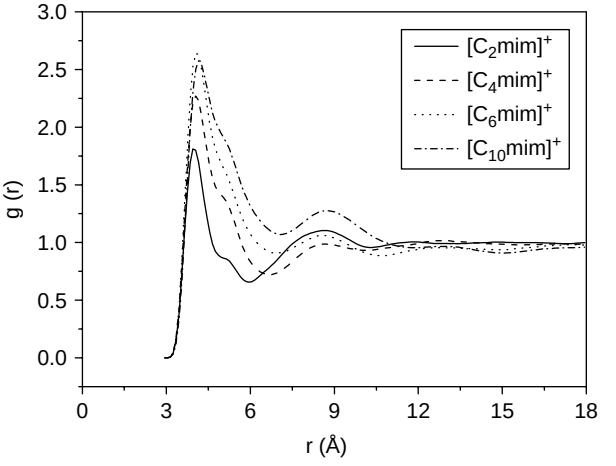

Figure 9. RDFs between the terminal carbon in $[C_n mim]^+$.

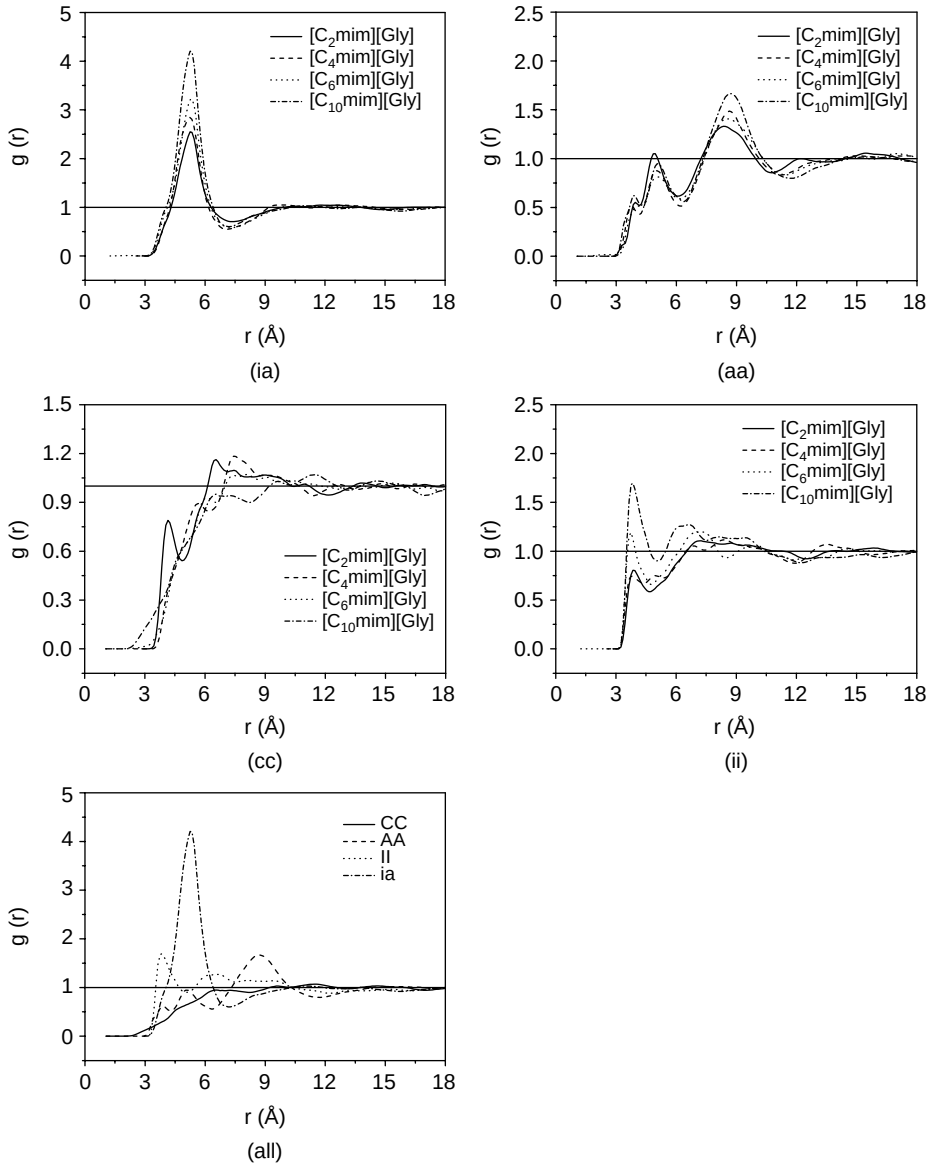

Figure 10. COM RDFs between anion–anion (aa), cation–cation (cc), imidazolium rings and themselves (ii), imidazolium rings and anions (ia).

The above result may be due to COM for the cations not being consistent with the centre of the imidazolium ring, especially for the long alkyl side chain. The RDFs for the COM of imidazolium rings, were calculated and are shown in Figure 10(ii). As shown in the figure, the RDF peak height for $[C_{10}mim][Gly]$ is the highest of all the four ILs. Compared with Figure 10(aa), it is obvious that the RDFs are very different, as there is only one obvious peak for each RDF at about 4 Å. In order to present the differences clearly, four kinds of COM RDFs for $[C_{10}mim][Gly]$ are shown in Figure 10(all) and compared with each other. After the first peak of RDFs for the anion–imidazolium ring, a clear peak is observed for the anion–anion RDF, and it should be the second shell. The result is similar to $[C_{12}mim][PF_6]$ [12]. However, there is an abnormal phenomenon that the first peak location of the RDF for the imidazolium ring and itself appears before that for the ia RDFs. Why does it happen? We suppose that there is a strong interaction between O2 in anion and H atoms in the imidazolium ring, and one $[Gly]^-$ would catch more than two cations. It can be proved by the spatial distribution functions (SDFs) in Figure 12. The anions are distributed at the above and below the imidazolium ring along the axis of the C—H bond, and the imidazolium rings are distributed at two sides of the ring. It is reported by Rogers et al. [35] that the imidazolium cations of $[C_1mim][PF_6]$ will form a weakly C—H…p hydrogen-bonded zigzag chain motif via CH_3. However, for our

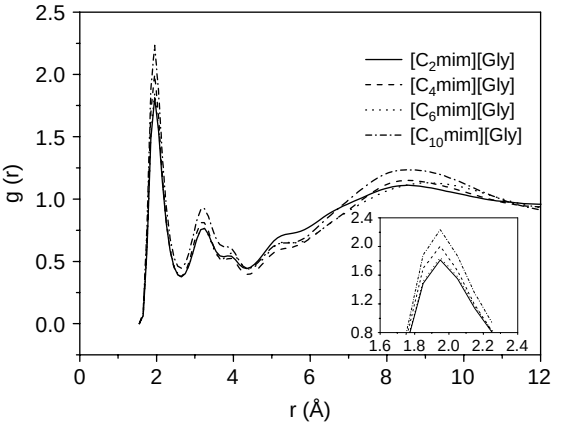

Figure 11. RDFs of O2—H in $[Gly]^-$.

system, the imidazolium rings of these cations may be aligned approximately parallel to each other (see Figure 13). So the distance between the rings is very close, even closer than that between the ring and anion.

5. Conclusions

A series of amino acid ILs were studied by molecular dynamics based on the all-atom force field. Simulations were carried out for four $[C_n mim][Gly]$ ILs at 298.15 K. Volume expansivity and heat capacity for $[C_2mim][Gly]$ were compared with the experimental data to validate the force field, and a good agreement was obtained.

The local structures and micro-interaction were studied by the RDFs. The site–site RDFs of the H atoms in cations and O2 in the anion reveal that the interaction decreases in the order of H5 > H4 > H1. For different ILs, the order is $[C_{10}mim]^+ > [C_6mim]^+ > [C_4mim]^+ > [C_2mim]^+$. The interaction between the alkyl chain

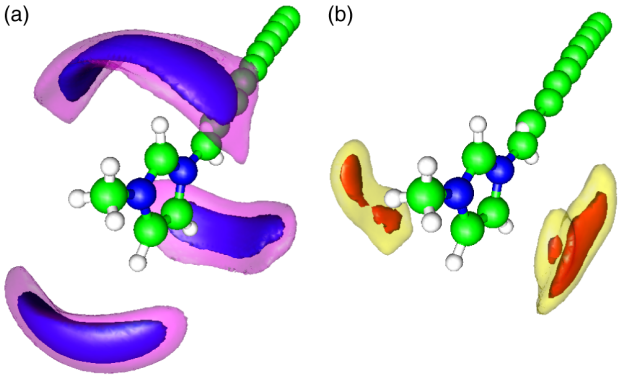

Figure 12. SDFs for (a) C in the anion around the imidazolium ring and (b) CR in the imidazolium ring around the imidazolium ring, and the atom type and location are shown in Figure 1. For part (a), the blue- and pink-bounded contour surfaces are drawn at 20 and 10 times the average density, respectively. For part (b), the orange- and yellow-bounded contour surfaces are drawn at 9 and 6 times the average density, respectively.

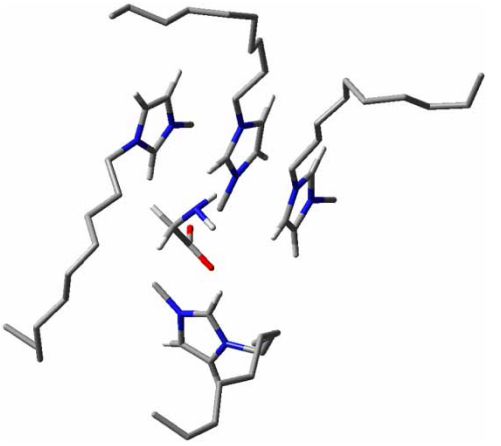

Figure 13. A snapshot of four cations and one anion in $[C_{10}mim][Gly]$ at 4 ns.

themselves was investigated in detail. It is found that aggregation of the alkyl chains could be observed in the ILs with alkyl side chains longer than or equal to C4. COM RDFs were also computed to study the ionic interaction. Because one terminal of $[Gly]^-$ is the electronic acceptor, and the other is the adopter, hydrogen bonds could form between anions themselves. A small peak is found before the highest one for anion–anion RDFs. RDFs for imidazolium rings were studied, and it is interesting to find that the first peak locations of RDFs for the imidazolium ring and itself appear before the imidazolium ring and anion RDFs. Through the SDFs, it is implied that the imidazolium rings of these cations may be aligned approximately parallel to each other. It is no surprise that the distance between the rings is very close, even closer than that between the ring and the anion.

Acknowledgements

This work was supported by the National Basic Research Program of China (2009CB219901), the National Science Fund of China for Distinguished Young Scholar (20625618) and the National Natural Scientific Fund of China (20903098).

References

[1] L.A. Blanchard, D. Hancu, E.J. Beckman, and J.F. Brennecke, *Green processing using ionic liquids and CO_2*, Nature 399 (1999), p. 28.
[2] R. Sheldon, *Catalytic reactions in ionic liquids*, Chem. Commun. 23 (2001), p. 2399.
[3] A.C. Cole, J.L. Jensen, I. Ntai, K.L.T. Tran, K.J. Weaver, D.C. Forbes, and J.H. Davis, Jr, *Novel Brønsted acidic ionic liquids and their use as dual solvent-catalysts*, J. Am. Chem. Soc. 124 (2002), p. 5962.
[4] J.S. Wilkes, *Short history of ionic liquids – From molten salts to neoteric solvents*, Green Chem. 4 (2002), p. 73.
[5] H. Gao, B. Han, J. Li, T. Jiang, Z. Liu, W. Wu, Y. Chang, and J. Zhang, *Preparation of room-temperature ionic liquids by neutralization of 1,1,3,3-tetramethylguanidine with acids and their use as media for mannich reaction*, Synth. Commun. 34 (2004), p. 3083.

[6] S. Zhang and X. Lu, *Ionic liquids: Form fundamentals to applications*, Science Press, Beijing, 2006.
[7] K. Fukumoto, M. Yoshizawa, and H. Ohno, *Room temperature ionic liquids from 20 natural amino acids*, J. Am. Chem. Soc. 127 (2005), p. 2398.
[8] J. Yang, Q. Zhang, B. Wang, and J. Tong, *Study on the properties of amino acid ionic liquid EMIGly*, J. Phys. Chem. B 110 (2006), p. 22521.
[9] J. Zhang, S. Zhang, Dong, Y. Zhang, Y. Shen, and X. Lv, *Supported absorption of CO_2 by tetrabutylphosphonium amino acid ionic liquids*, Eur. J. Chem. 12 (2006), p. 4021.
[10] T.I. Morrow and E.J. Maginn, *Molecular dynamics study of the ionic liquid 1-n-butyl-3-methylimidazolium hexafluorophosphate*, J. Phys. Chem. B 106 (2002), p. 12807.
[11] J.N.A.C. Lopes and A.A.H. Pádua, *Molecular force field for ionic liquids composed of triflate or bistriflylimide anions*, J. Phys. Chem. B 108 (2004), p. 16893.
[12] J.N.A.C. Lopes and A.A.H. Pádua, *Nanostructural organization in ionic liquids*, J. Phys. Chem. B 110 (2006), p. 3330.
[13] M.G.D. Pópolo and G.A. Voth, *On the structure and dynamics of ionic liquids*, J. Phys. Chem. B 108 (2004), p. 1744.
[14] Z. Liu, S. Huang, and W. Wang, *A refined force field for molecular simulation of imidazolium-based ionic liquids*, J. Phys. Chem. B 108 (2004), p. 12978.
[15] C. Cadena, Q. Zhao, R.Q. Snurr, and E.J. Maginn, *Molecular modeling and experimental studies of the thermodynamic and transport properties of pyridinium-based ionic liquids*, J. Phys. Chem. B 110 (2006), p. 2821.
[16] X. Liu, S. Zhang, G. Zhou, G. Wu, X. Yuan, and X. Yao, *New force field for molecular simulation of guanidinium-based ionic liquids*, J. Phys. Chem. B 110 (2006), p. 12062.
[17] X. Liu, G. Zhou, S. Zhang, G. Wu, and G. Yu, *Molecular simulation of guanidinium-based ionic liquids*, J. Phys. Chem. B 111 (2007), p. 5658.
[18] J. de Andrade, E.S. Böes, and H. Stassen, *A force field for liquid state simulations on room temperature molten salts: 1-Ethyl-3-methylimidazolium tetrachloroaluminate*, J. Phys. Chem. B 106 (2002), p. 3546.
[19] N.M. Micaelo, A.M. Baptista, and C.M. Soares, *Parametrization of 1-butyl-3-methylimidazolium hexafluorophosphate/nitrate ionic liquid for the GROMOS force field*, J. Phys. Chem. B 110 (2006), p. 14444.
[20] A. Chaumont, E. Engler, and G. Wipff, *Uranyl and strontium salt solvation in room-temperature ionic liquids. A molecular dynamics investigation*, Inorg. Chem. 42 (2003), p. 5348.
[21] Y. Wang and G.A. Voth, *Unique spatial heterogeneity in ionic liquids*, J. Am. Chem. Soc. 127 (2005), p. 12192.
[22] B.L. Bhargava and S. Balasubramanian, *Layering at an ionic liquid? vapor interface: A molecular dynamics simulation study of [bmim][PF6]*, J. Am. Chem. Soc. 128 (2006), p. 10073.
[23] C. Cadena, J.L. Anthony, J.K. Shah, T.I. Morrow, J.F. Brennecke, and E.J. Maginn, *Why is CO_2 so soluble in imidazolium-based ionic liquids?* J. Am. Chem. Soc. 126 (2004), p. 5300.
[24] K.E. Gutowski and E.J. Maginn, *Amine-functionalized task-specific ionic liquids: A mechanistic explanation for the dramatic increase in viscosity upon complexation with CO_2 from molecular simulation*, J. Am. Chem. Soc. 130 (2008), p. 14690.
[25] G. Zhou, X. Liu, S. Zhang, G. Yu, and H. He, *A force field for molecular simulation of tetrabutylphosphonium amino acid ionic liquids*, J. Phys. Chem. B 111 (2007), p. 7078.
[26] C.I. Bayly, P. Cieplak, W.D. Cornell, and P.A. Kollman, *A well-behaved electrostatic potential based method using charge restraints for deriving atomic charges: the RESP model*, J. Phys. Chem. 97 (1993), p. 10269.
[27] W.D. Cornell, P. Cieplak, C.I. Bayly, I.R. Gould, K.M. Merz, Jr, D.M. Ferguson, D.C. Spellmeyer, T. Fox, J.W. Caldwell, and P.A. Kollman, *A second generation force field for the simulation of proteins, nucleic acids, and organic molecules*, J. Am. Chem. Soc. 117 (1995), p. 5179.
[28] M.P. Allen and D.J. Tildesley, *Computer Simulations of Liquids*, Clarendon Press, Oxford, 1987.
[29] A.P. Lyubartsev and A. Laaksonen, *M.DynaMix – A scalable portable parallel md simulation package for arbitrary molecular mixtures*, Comput. Phys. Commun. 128 (2000), p. 565.
[30] G.J. Martyna, M.E. Tuckerman, D.J. Tobias, and M.L. Klein, *Explicit reversible integrators for extended system dynamics*, Mol. Phys. 87 (1996), p. 1117.
[31] M. Tuckerman, B.J. Berne, and G.J. Martyna, *Reversible multiple time scale molecular dynamics*, J. Chem. Phys. 97 (1992), p. 1990.
[32] S.W. Deleeuw, J.W. Perram, and E.R. Smith, *Simulation of electrostatic systems in periodic boundary conditions. III. Further theory and applications*, Proc. R. Soc. Lond. A: Math. Phys. Eng. Sci. 388 (1983), p. 177.
[33] S. Zhang, N. Sun, X. He, X. Lu, and X. Zhang, *Physical properties of ionic liquids: Database and evaluation*, J. Phys. Chem. Ref. Data 35 (2006), p. 1475.
[34] M. Lagache, P. Ungerer, A. Boutina, and A.H. Fuchsa, *Prediction of thermodynamic derivative properties of fluids by Monte Carlo simulation*, Phys. Chem. Chem. Phys. 3 (2001), p. 4333.
[35] J.D. Holbrey, W.M. Reichert, N. Mark, O. Sheppard, C. Hardacrebc, and R.D. Rogers, *Liquid clathrate formation in ionic liquid–aromatic mixtures*, Chem. Commun. 21(4) (2003), p. 476.